Acta Universitatis Sapientiae
Electrical and Mechanical Engineering, 10 (2018) 20-41

DOI: 10.2478/auseme-2018-0002

Model Predictive Control of a Differential-Drive Mobile Robot

Samir BOUZOUALEGH[1], El-Hadi GUECHI[1] and Ridha KELAIAIA[2]

[1] Laboratoire d'Automatique de Skikda (LAS), Faculté de Technologie, Département de Génie Électrique, Université 20 Août 1955-Skikda, BP 26, Route El-Hadaeik, Skikda 21000, Algeria,
e-mail: samir.bouzoualegh@gmail.com, e.guechi@univ-skikda.dz
[2] Faculty of Technology, Université de 20 Août 1955-Skikda,
e-mail: r.kelaiaia@univ-skikda.dz

Manuscript received September 22, 2018; revised December 10, 2018.

Abstract: This paper presents a model predictive control (MPC) for a differential-drive mobile robot (DDMR) based on the dynamic model. The robot's mathematical model is nonlinear, which is why an input–output linearization technique is used, and, based on the obtained linear model, an MPC was developed. The predictive control law gains were acquired by minimizing a quadratic criterion. In addition, to enable better tuning of the obtained predictive controller gains, torques and settling time graphs were used. To show the efficiency of the proposed approach, some simulation results are provided.

Keywords: mobile base; dynamic model; nonlinear control; model predictive control; input-output linearization.

1. Related works

In general, the control of mobile robots poses a very strong challenge among the robot control community. Today, several studies are still ongoing, especially in aeronautical space exploration, the inspection of nuclear power plants, and automated agriculture, motivating the increasing interest in mobile robotics [1]. Such applications need to find an adequate control law for mobile robots after taking into consideration all the possible constraints. For control purposes, many approaches are available in the literature; for example, Guechi et al. [2] developed predictive control dynamics for a two-link manipulator robot. The idea consists of linearizing the nonlinear dynamic model of the robot through feedback linearization, and, based on the obtained linear model, an MPC was developed by assuming the outputs of the predictive controller as constant in the prediction horizon interval. A similar idea was exploited by Belda et al. [3] but with a different model presentation; as they designed a model predictive control (MPC) for an autonomous mobile robot system with a 5-DOF manipulator arm.

Based on the manipulator robot dynamic model, the nonlinear state space model is converted into a linear model by considering the time-varying matrices as constants within one prediction horizon. Another application of [3] was intended for mobile platforms; Kamel et al. [4] applied a combination of linear model predictive control and input–output feedback linearization for a team of wheeled mobile robots to accomplish a formation task. The time-variant matrix of the state space model was considered as a constant matrix between the prediction intervals. Guechi et al. [5] did a comparative study between a MPC and Linear Quadratic (LQ) optimal control of a two-link robot arm, and the simulation results showed that the proposed MPC gave a better system performance then the LQ optimal control approach. Elkhateeb [6] developed a novel tuning methodology of a PID controller for trajectory tracking of a manipulator robot. The optimal gains of the PID controller are obtained by using a dynamic inertia weight artificial bee colony optimization algorithm. Mendili et al. [7], [8] presented two papers, the first of which was a predictive controller of a holonomic omnidirectional mobile robot. The predictive control law was obtained by using a state space model, which is based on the robot dynamic model. The simulation results illustrated the effectiveness of the control law joined with the dynamic model. Meanwhile, the second paper was an application of the model predictive control to solve the problem of the trajectory tracking and path following of an omnidirectional mobile robot. Two different models were considered: the kinematic and the dynamic model. The results showed the effectiveness of the dynamic model in comparison with the kinematic one in tracking the trajectory and path without posture. To achieve better path tracking for a wheeled mobile robot (WMR), Maniatopoulos et al. [9] developed an MPC-based solution to the problem of navigating a non-holonomic mobile robot while maintaining visibility. The proposed approach combines the convergence properties of a dipolar vector field along with a constrained nonlinear MPC formulation using recentered barrier functions, which take into account the visibility constraints and the saturation of control inputs. The control strategy falls into the class of dual-mode MPC schemes. That is, the system trajectories are forced by the model predictive controller into a suitably defined terminal region containing the goal configuration. In this region, the trajectories resulting from tracking the dipolar vector field by construction do not violate the visibility constraints. To achieve better path tracking for a wheeled mobile robot (WMR), Sinaeefar et al. [10] developed an adaptive fuzzy nonlinear model predictive control (NMPC). The proposed controller solves the integrated kinematic and dynamic tracking problem in the presence of both parametric and non-parametric uncertainties. Furthermore, a fuzzy system, the parameters of which are updated online by a gradient descent algorithm, is employed. While this fuzzy system can provide an appropriate

model for the robot, it can also deal with any changes in robot parameters. Mazur [11] presented a general solution to the path-following problem for mobile manipulators with a non-holonomic mobile platform. New proposed control algorithms – for mobile manipulators with fully known dynamics or with parametric uncertainty in the dynamics – take into consideration the kinematics as well as the dynamics of the non-holonomic mobile manipulator. The convergence of the control algorithms was proved using LaSalle's invariance principle. Ostafew et al. [12] developed a learning-based nonlinear model predictive control algorithm for a path-repeating mobile robot negotiating large-scale, GPS-denied outdoor environments. The disturbance is modelled as a Gaussian process based on observed disturbances as a function of relevant variables, such as the system state and input. Localization for the controller is provided by an on-board visual teach and repeat mapping and navigation system. Two experiments on two significantly different robots demonstrated the system's ability to handle unmodelled terrain and robot dynamics and a speed scheduler based on previous experience to address the classic exploration vs. exploitation trade-off, balancing speed and path-tracking errors. Mitrovic et al. [13] presented a new methodology for the avoidance of one or more obstacles for the navigation of a differential-drive mobile robot. The approach is based on fuzzy logic with virtual fuzzy magnets and represents a reactive controller for navigation through an unknown environment. The relative parameters of the obstacle in the robot's way are determined at the preprocessing stage, and the algorithm is therefore applicable to obstacles of different sizes. The algorithm, designed to avoid a single stationary obstacle, was generalized and successfully applied in a multiple-obstacle navigation scenario. The efficiency of the algorithm was illustrated by computer simulations using the kinematic model of a mobile robot.

This paper proposes a novel approach to controlling a differential-drive mobile robot. The control strategy of this approach is to linearize the DDMR dynamic model by using an input–output linearization control in the first step; then, the second step is to develop an MPC for the obtained linear model by minimizing a quadratic criterion.

This paper is organized as follows. In the second section, we provide a description of the DDMR and its different models. In the third section, the control strategy for the DDMR from an initial position up to a final position using a model predictive control (MPC) is presented. The simulation results are presented in the fourth section.

2. Differential drive mobile robot models

A differential drive mobile robot can be presented as depicted in *Fig.1*.

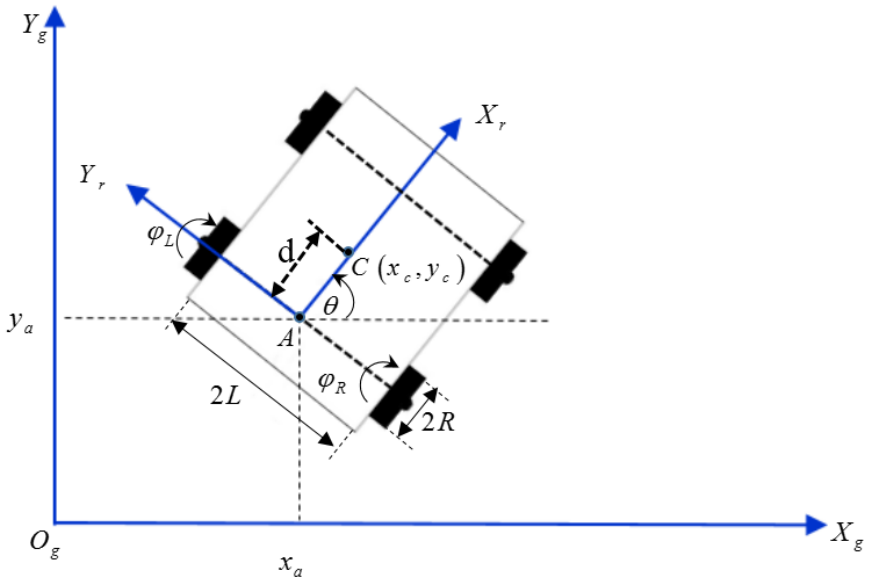

Figure 1: Schematic representation of a DDMR robot.

A. Coordinate systems

To describe the mobile robot's position, we have defined two coordinate systems:

A.1. Global coordinate system: This coordinate system is a global frame which is fixed in the environment in which the DDMR moves in. and is denoted as $\{X_g, Y_g\}$.

A.2. Robot coordinate system: This coordinate system is a local frame attached to the DDMR, and thus, moving with it. And is denoted as $\{X_r, Y_r\}$.

The two defined frames are shown in *Fig.1* the origin of the robot frame is defined to be the mid-point A on the axis between the wheels. The center of mass C of the robot is assumed to be on the axis of symmetry, at a distance d from the origin A.

The mobile robot position and orientation in the global Frame can be defined as:

$$q^g = \left| x_a \quad y_a \quad \theta \right|^T \tag{1}$$

B. Kinematic constraints of DDMR

The DDMR motion is characterized by the non-holonomic constraints equations, which are based on the following assumptions [14]:

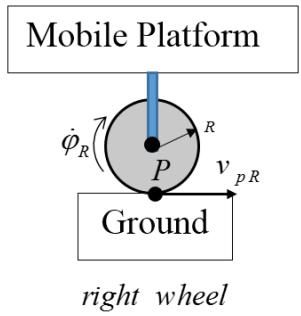

Figure 2: Rolling motion constraints.

- *No lateral slip*:

$$-x_a \cos\theta + y_a \sin\theta = 0 \tag{2}$$

- *Pure rolling*:

$$\begin{cases} \dot{x}_{PR} \cos\theta + \dot{y}_{PR} \sin\theta = R\dot{\phi}_R \\ \dot{x}_{PL} \cos\theta + \dot{y}_{PL} \sin\theta = R\dot{\phi}_L \end{cases} \tag{3}$$

$$\begin{cases} \dot{x}_{PR} = \dot{x}_{PL} = \dot{x}_a + L\dot{\theta}\cos\theta \\ \dot{y}_{PR} = \dot{y}_{PL} = \dot{y}_a + L\dot{\theta}\sin\theta \end{cases} \tag{4}$$

where: $\dot{\phi}_R$ and $\dot{\phi}_L$ are the right and left wheels angular velocities respectively, R is the wheels' radius, L is the distance between the driving wheels and the axis of symmetry and d is the distance between the points A and C.

Taking (4) into account, (3)becomes the following:

$$\begin{cases} \dot{x}_a \cos\theta + \dot{y}_a \sin\theta + L\dot{\theta} - R\dot{\phi}_R = 0 \\ \dot{x}_a \cos\theta + \dot{y}_a \sin\theta - L\dot{\theta} - R\dot{\phi}_L = 0 \end{cases} \tag{5}$$

The constraint equations (2) and (4) can be presented as follow:

$$\Lambda(q)\dot{q} = 0 \tag{6}$$

where:
$$\Lambda(q) = \begin{bmatrix} -\sin\theta & \cos\theta & 0 & 0 & 0 \\ \cos\theta & \sin\theta & L & -R & 0 \\ \cos\theta & \sin\theta & -L & 0 & -R \end{bmatrix} \tag{7}$$

$$\dot{q} = \begin{bmatrix} \dot{x}_a & \dot{y}_a & \dot{\theta} & \dot{\phi}_R & \dot{\phi}_L \end{bmatrix}^T \tag{8}$$

C. Kinematic model

Kinematic modelling is the study of the motion of mechanical systems without considering the forces that affect the motion.

We can calculate the linear and angular velocities for the driving wheels in the robot frame as below:

$$v = \frac{v_{pR} + v_{pL}}{2}, w = \frac{v_{pR} - v_{pL}}{2L} \tag{9}$$

where v_{pR} and v_{pL} Are the right and left linear velocities of the contact point P.

Therefore, the platform centre A velocities in the robot and global frames are as follows:

$$\dot{q}^r = \begin{bmatrix} \dot{x}_a^r \\ \dot{y}_a^r \\ w \end{bmatrix} = \frac{R}{2} \begin{bmatrix} 1 & 1 \\ 0 & 0 \\ \frac{1}{L} & -\frac{1}{L} \end{bmatrix} \begin{bmatrix} \dot{\phi}_R \\ \dot{\phi}_L \end{bmatrix}, \tag{10}$$

$$\dot{q}^g = \begin{bmatrix} \dot{x}_a^r \\ \dot{y}_a^r \\ w \end{bmatrix} = \frac{R}{2} \begin{bmatrix} \cos\theta & \cos\theta \\ \sin\theta & \sin\theta \\ \frac{1}{L} & -\frac{1}{L} \end{bmatrix} \begin{bmatrix} \dot{\phi}_R \\ \dot{\phi}_L \end{bmatrix} \tag{11}$$

D. Dynamic model

Dynamics is the study of mechanical system motion taking into consideration the different forces that affect it. The dynamic model of the DDMR is essential for simulation analysis of its motion and for the design of various motion control algorithms using the Lagrange formula:

$$\frac{d}{dt}\left(\frac{\partial L}{\partial \dot{q}_i}\right)+\frac{\partial L}{\partial q_i}=F-\Lambda^T\left(q\right)\lambda \tag{12}$$

where L=T-V, T is the kinematic energy, V is the potential energy of the mobile platform, q_i are the generalized coordinates, F is the generalized force vector, Λ is the constraint matrix, and λ is the Lagrange multiplier vector associated with the constraints. In addition, knowing the DDMR kinetic energy, which is the sum of T_c, the kinetic energy of the robot platform without wheels, plus T_{wR},T_{wL}, the kinetic energy of the wheels, note that their formulas are as follows[14]:

$$\begin{cases} T_c=\frac{1}{2}m_c v_M^2+\frac{1}{2}I_c\dot{\theta}^2 \\ T_{wR}=\frac{1}{2}m_w v_{wR}^2+\frac{1}{2}I_m\dot{\theta}^2+\frac{1}{2}I_w\dot{\phi}_R^2 \\ T_{wL}=\frac{1}{2}m_w v_{wL}^2+\frac{1}{2}I_m\dot{\theta}^2+\frac{1}{2}I_w\dot{\phi}_L^2 \end{cases} \tag{13}$$

where m_c and I_c are the mass and the moment of inertia of the platform without the driving wheels, respectively, m_w and I_w are the mass and the moment of inertia of each driving wheel plus the rotor of its motor.

The dynamic model of the non-holonomic DDMR with n generalized coordinates $(q_1,q_2,...,q_n)$ and subject to *m* constraints can be described by the following equation of motion [15]:

$$M\left(q\right)\ddot{q}+V\left(q,\dot{q}\right)\dot{q}=B\left(q\right)\tau-\Lambda^T\left(q\right)\lambda \tag{14}$$

$M\left(q\right)$: the inertia moment matrix, symmetric positive definite matrix.

$V\left(q,\dot{q}\right)$: the Coriolis and centrifugal matrix.

$B\left(q\right)$: input matrix.

τ : input vector.

In addition:

$$M(q)=\begin{bmatrix} m_T & 0 & -m_T d\sin\theta & 0 & 0 \\ 0 & m_T & m_T d\cos\theta & 0 & 0 \\ -m_T d\sin\theta & m_T d\cos\theta & I & 0 & 0 \\ 0 & 0 & 0 & I_w & 0 \\ 0 & 0 & 0 & 0 & I_w \end{bmatrix} \tag{15}$$

$$V(q,\dot{q})=\begin{bmatrix} 0 & -m_T d\dot{\theta}\cos\theta & 0 & 0 & 0 \\ 0 & -m_T d\dot{\theta}\sin\theta & 0 & 0 & 0 \\ 0 & 0 & 0 & 0 & 0 \\ 0 & 0 & 0 & 0 & 0 \\ 0 & 0 & 0 & 0 & 0 \end{bmatrix} \tag{16}$$

$$B(q)=\begin{vmatrix} 0 & 0 & 0 & 1 & 0 \\ 0 & 0 & 0 & 0 & 1 \end{vmatrix}^T \tag{17}$$

Note that:

$$m_T = m_c + 2m_w, \quad I = I_c + m_c d^2 + 2m_w L^2 + 2I_m \tag{18}$$

For the purpose of control and simulation and because the Lagrange multipliers λ_i are unknown, it is more convenient to eliminate the constraint term $\Lambda(q)^T\lambda$ in (14). Furthermore, since the constrained velocity is always in the null space of $\Lambda(q)$, it is possible to define $(n-m=2)$ velocities $\eta(t)=[\eta_1\ \eta_2\ ]$, such that [15]:

$$\dot{q} = S(q)\eta(t) \tag{19}$$

We can verify that $S(q)$ is also the null space of the constraint matrix $\Lambda(q)$, which means: $S(q)\Lambda(q)=0$; then, it is easy to verify that:

$$S(q)=\begin{bmatrix} \frac{R}{2L}(L\cos\theta - d\sin\theta) & \frac{R}{2L}(L\cos\theta + d\sin\theta) \\ \frac{R}{2L}(L\sin\theta + d\cos\theta) & \frac{R}{2L}(L\sin\theta - d\cos\theta) \\ \frac{R}{2L} & -\frac{R}{2L} \\ 1 & 0 \\ 0 & 1 \end{bmatrix} \tag{20}$$

Therefore based on $S(q)$ matrix choice, and the state variable $q=\begin{bmatrix} x_a & y_a & \theta & \phi_R & \phi_L \end{bmatrix}^T$ we have $\eta(t)=[\dot{\phi}_R \ \dot{\phi}_L\ ]$. By differentiating (19) and substituting the expression of $\ddot{q}$ into (14) and multiplying it by S^T, the dynamic model equation is as follow [14]:

$$\bar{M}\,\dot{\eta}+\bar{V}=\bar{B}\,\tau=\tau \tag{21}$$

Thus:

$$\begin{cases} \bar{M}=S^T(q)M(q)S(q) \\ \bar{V}=S^T(q)\left(M(q)\dot{S}(q)+V(q,\dot{q})S(q)\right) \\ \bar{B}=S^T(q)B(q)=\mathrm{I}_{2\times 2} \end{cases} \tag{22}$$

(21) shows that the DDMR dynamic model is a function only of the right and left wheel angular velocities $(\dot{\phi}_R,\dot{\phi}_L)$, the robot angular velocity $\dot{\theta}$ and the driving motor torques (τ_R,τ_L).

3. Control algorithm

In this part, a predictive control law for a differential-drive mobile robot is developed. First, we consider the nonlinear dynamic model given by (21) Then, we convert the nonlinear dynamic model into a completely linear model on which the linear control approach is applied. Once the linear model has been obtained, a model predictive control will be designed in the second step [15].

3.A Input-output linearization

Let consider the state space vector below:

$$x=[q^T\ \eta^T\ ]^T=[x_c,y_c,\theta,\phi_R,\phi_L,\dot{\phi}_R,\dot{\phi}_R\ ]^T \tag{23}$$

We can write the state space dynamic model as follows:

$$\dot{x}=\begin{bmatrix} S\eta \\ 0 \end{bmatrix}+\begin{bmatrix} 0 \\ \bar{M}^{-1}\left(\tau-\bar{V}\right) \end{bmatrix}=\begin{bmatrix} S\eta \\ 0 \end{bmatrix}+\begin{bmatrix} 0 \\ I_{2x2} \end{bmatrix}\bar{M}^{-1}\left(\tau-\bar{V}\right) \tag{24}$$

We can rewrite the above state space equation as follow:

$$\dot{x}=f(x)+g(x)u \tag{25}$$

where:

$$\begin{cases} u = \bar{M}^{-1}\left(\tau - \bar{V}\right) \\ f\left(x\right) = \begin{bmatrix} S\eta \\ 0 \end{bmatrix} \\ g\left(x\right) = \begin{bmatrix} 0 \\ I_{2\times 2} \end{bmatrix} \end{cases} \tag{26}$$

From (25), we could assume a new input u which could linearize(24), but the challenge now is to find another equation that links the new input u with the robot's position in such a way that we can compute the wheels' torques based on this new input.

Let us suppose $y = \Upsilon(q) = \begin{bmatrix} x_c & y_c \end{bmatrix}^T$ is the output vector that we need to control, as shown in *Fig. 2*.

$$\begin{bmatrix} x_c \\ y_c \end{bmatrix} = \begin{bmatrix} x_a \\ y_a \end{bmatrix} + \begin{bmatrix} x_c^a & -y_c^a \\ x_c^a & y_c^a \end{bmatrix} \begin{bmatrix} \cos\theta \\ \sin\theta \end{bmatrix} \tag{27}$$

x_c^a, y_c^a are the coordinates of point C in the robot frame. Therefore:

$$\dot{y} = \partial\Upsilon/\partial t = \left(\partial\Upsilon/\partial q\right)\dot{q} = J_f\left[S\left(q\right)\eta\left(t\right)\right] = \left[J_f S\left(q\right)\right]\eta\left(t\right) = \Gamma\left(q\right)\eta\left(t\right) \tag{28}$$

Γ : 2x2 decoupling matrix, such as $\Gamma = \begin{bmatrix} \Gamma_{11} & \Gamma_{12} \\ \Gamma_{21} & \Gamma_{22} \end{bmatrix}$,

where:

$$\begin{bmatrix} \Gamma_{11} \\ \Gamma_{12} \\ \Gamma_{21} \\ \Gamma_{22} \end{bmatrix} = \frac{R}{2L} \begin{bmatrix} \mathrm{L} - y_c^a & -d - x_c^a \\ \mathrm{L} + y_c^a & d + x_c^a \\ \mathrm{L} - y_c^a & d + x_c^a \\ \mathrm{L} + y_c^a & -d - x_c^a \end{bmatrix} \begin{bmatrix} \cos\theta \\ \sin\theta \end{bmatrix} \tag{29}$$

The second derivate of (28), is obtained as follows:

$$\ddot{y} = \dot{\Gamma}\eta + \Gamma\dot{\eta} \tag{30}$$

As developed in [15], to make Eq. (30) linear we have to do the following substitution:

$$\begin{cases} \ddot{y} = v \\ \dot{\eta} = u \end{cases} \tag{31}$$

which is the I/O feedback linearisation, therefore the second input u will be:

$$v = \dot{\Gamma}\eta + \Gamma u \Rightarrow u = \Gamma^{-1}(v - \dot{\Gamma}\eta) \tag{32}$$

By substituting the second input u of the Eq.(32) into Eq. (21), we can compute the DDMR wheels' torques as follows:

$$\tau = \bar{M}u + \bar{\mathrm{V}} \tag{33}$$

Now we need to find out the variable v , note that:

$$\ddot{y} = \begin{bmatrix} \ddot{x}_c \\ \ddot{y}_c \end{bmatrix} = \begin{bmatrix} v_1 \\ v_2 \end{bmatrix} \tag{34}$$

where: $v = [v_1, v_2]$ is the synthetic control vector. This will be the subject of the following subsection.

3.B Model Predictive Control law

Following the I/O feedback linearization, let us apply the model predictive control to compute the first input v_1, where v_i is the synthetic control vector. Now let us develop the predictive control law for the x_c coordinate, which will be similar to the y_c coordinate.

$$\begin{cases} \dot{x}_1(t) = x_2(t) \\ \dot{x}_2(t) = v_1(t) \\ z(t) = x_1(t) \end{cases} \tag{35}$$

where: $[x_1 \quad x_2]^{\mathrm{T}} = [x_c \quad \dot{x}_c]^{\mathrm{T}}$, v_1 is the synthetic control of the x_c variable, while $z(t) = x_c(t)$ is the output signal.

Let consider that $v(t) = v_1$ is constant in the time interval [t t + h] [16-18] where h is the prediction horizon time, and by using the Eq.(35), we can formulate the prediction model as follows:

$$x_c(t+h) = \frac{1}{2} v_1 h^2 + \dot{x}_c(t)h + x_c(t) \tag{36}$$

We want to minimize not only the articulation deviation error but also the energy needed by the manipulator arm to reach the final position, which is why we choose the following cost function:

$$J = e_1^2(t+h) + \rho \int_t^{t+h} v^2 dt \tag{37}$$

where: $e_1(t+h) = x_{cd} - x_c(t+h)$ is the prediction error and x_{cd} is the desired value generated by the referenced trajectory. The horizon time h and the weight factor ρ are both positive parameters to be computed later.

By replacing the predicted value of $x_c(t+h)$ given by (36) into (37), therefore the criterion J become:

$$\begin{aligned} J = {} & x_{cd}^2 - x_{cd} v_1 h^2 - 2h x_{cd} \dot{x}_c(\mathrm{t}) - 2x_{cd} x_c(\mathrm{t}) + \frac{1}{4} v_1^2 h^4 + \\ & v_1 h^3 x_{cd} + v_1 h^2 x_c(\mathrm{t}) + \dot{x}_c^2(\mathrm{t}) h^2 + 2h\dot{x}_c(\mathrm{t}) x_c(\mathrm{t}) + x_c^2(\mathrm{t}) + \rho h v_1^2 \end{aligned} \tag{38}$$

Therefore: $\min\{J\}_{v_1}$ with subject to $h > 0$ and $\rho > 0$

$$\Rightarrow v_1(t) = k_1(x_{cd}(\mathrm{t}) - x_c(t)) - k_2 \dot{x}_c(t) \tag{39}$$

where the predictive control law gains are : $k_1 = \dfrac{2h}{h^3 + 4\rho}$ and $k_2 = \dfrac{2h^2}{h^3 + 4\rho}$.

The block diagram of the closed-loop system can be presented as shown in *Fig. 3*.

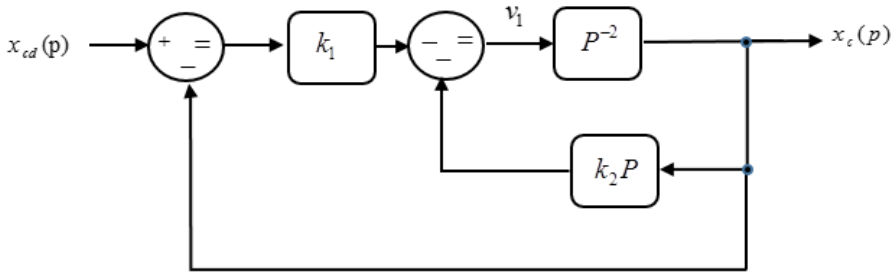

Figure 3: Closed-loop system.

Regarding the response of the equivalent system, we want it to adopt similar behavior to the second-order system: $\frac{w_0^2}{p^2 + 2\xi w_0 p + w_0^2}$, where ξ and w_0 are respectively the damping factor and the natural frequency.

The closed loop transfer function of the system shown in *Fig. 3* is given by:

$$\frac{x_c(p)}{x_{cd}(p)} = \frac{k_1}{p^2 + k_2 p + k_1} \tag{40}$$

we can verify that:

$$\begin{cases} 2\xi w_0 = \dfrac{2h^2}{h^3 + 4\rho} = hk \\ w_0^2 = \dfrac{2h}{h^3 + 4\rho} \end{cases} \tag{41}$$

Therefore:

$$h = \frac{2\xi}{w_0}, \quad \rho = \frac{\xi}{w_0^3}\left(1 - 2\xi^2\right) \tag{42}$$

The weight factor $\rho > 0$; therefore, from Eq.(42), as the damping factor ξ must be less than $1/\sqrt{2}$ to obtain good damping, we have to choose ξ as near as possible to $1/\sqrt{2}$; let us suppose $\xi = 0.999/\sqrt{2}$.

We want to find the h and ρ values in such a way that our system fulfills the following conditions:

$$\left|\tau_i\right| \le 150 Nm \,, i = 1,2. \text{ and } \quad T_{r\pm 5\%} \le 1s \tag{43}$$

with:

$$T_{r\pm 5\%} = \frac{-\ln(0.05\sqrt{1-\xi^2})}{\xi \, w_0} \text{ [19]} \tag{44}$$

Hence, we calculate and draw the maximum and minimum torque values (for each driving wheel) and the settling time values for several values of w_0 (from 1 rad/s to 10 rad/s), with a Matlab script obtained from the graphs below.

From *Fig. 4*, to have the maximum wheel torque less than or equal to 150 Nm, the natural frequency w_0 should be less than or equal to 9 rad/s. From *Fig. 5*, to have the minimum wheel torque greater than or equal to 150 Nm, the natural frequency w_0 should be less than or equal to 9 rad/s. In addition, from

Fig. 6, to have a settling time $T_{r\pm 5\%}$ less than or equal to 1 s, the natural frequency w_0 should be greater than or equal to 4.8 rad/s. Finally, the natural frequency w_0 should verify the following inequality:

$$4.8 rd/s \le w_0 \le 9 rd/s \tag{45}$$

Let us take $w_0 = 9$ rad/s, which means that $h = 0.157$ s, $\rho = 1.9.10^{-6}$ and the predictor control law gains values are $k_1 = 72.26$ and $k_2 = 12$.

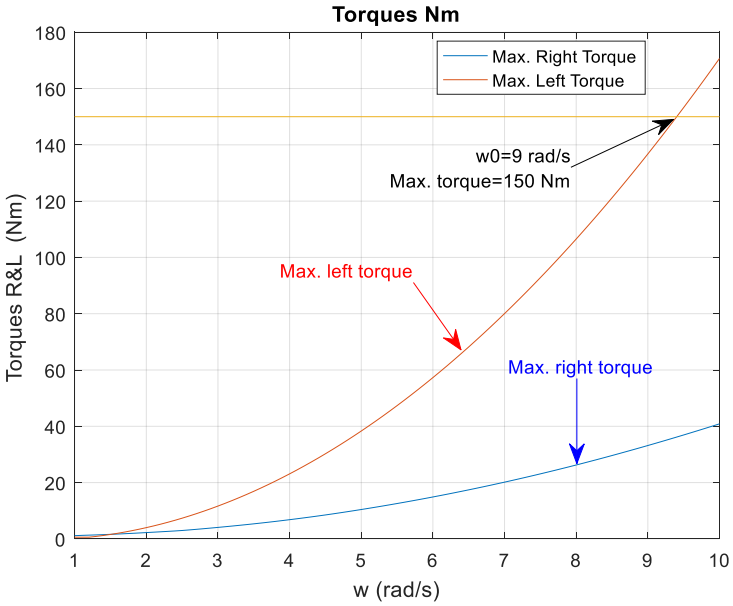

Figure 4: Max. torque $\tau_{i\max}$.

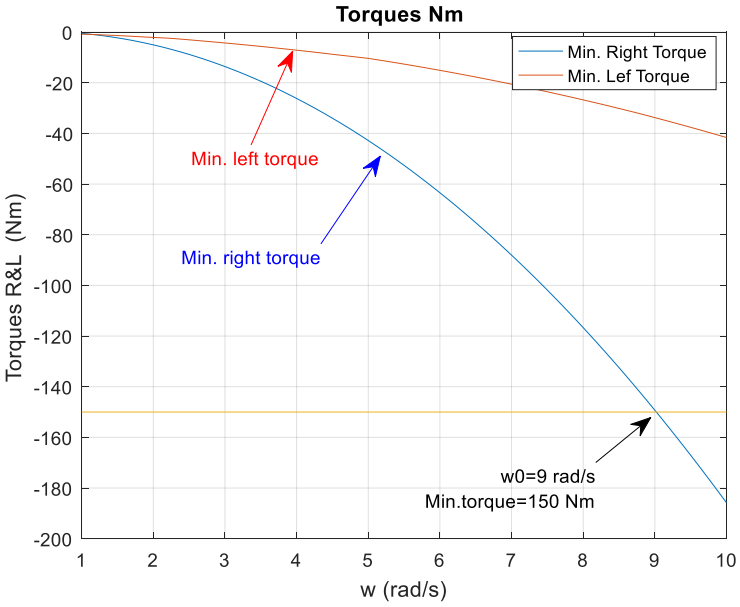

Figure 5: Max. torque $\tau_{i\,\min}$.

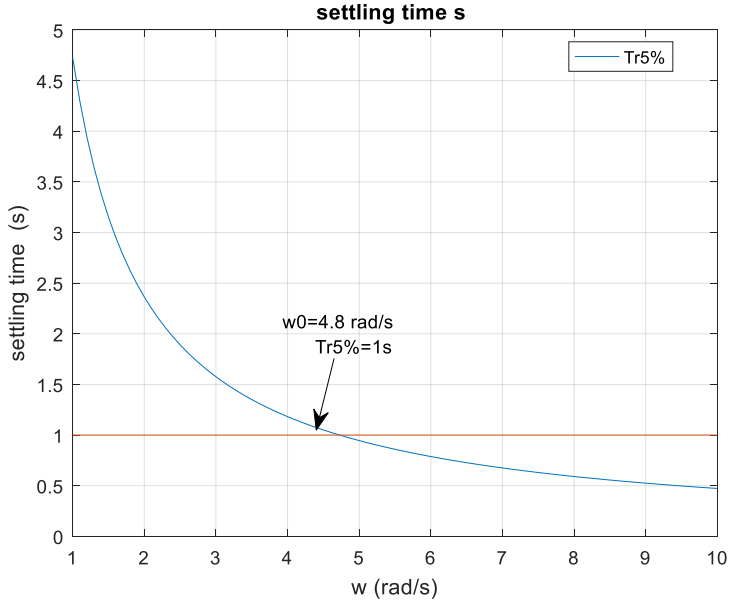

Figure 6: Max. torque $T_{r\pm5\%}$.

4. Simulation results

To show the suitability of our tinning parameters, k1 and k2, let us consider $m_c = 1(kg)$ and $I_c = 1(Nm^2)$ the mass and the moment of inertia of the platform without the driving wheels. $m_w = 0.1(kg)$ and $I_w = 0.1(Nm^2)$:the mass and the moment of inertia of each driving wheel plus the rotor of its motor. $I_m = 0.1(Nm^2)$: the moment of inertia of each wheel and the motor rotor.

For trajectory generation, we show that the DDMR moves from an initial point $P_{init} = (1,1)$ to a desired position $P_{dis} = (40,60)$ during a time period of 60 s, following a short distance, which will be a straight line; note that we suppose that there is no obstacle between P_{init} and P_{dis} .

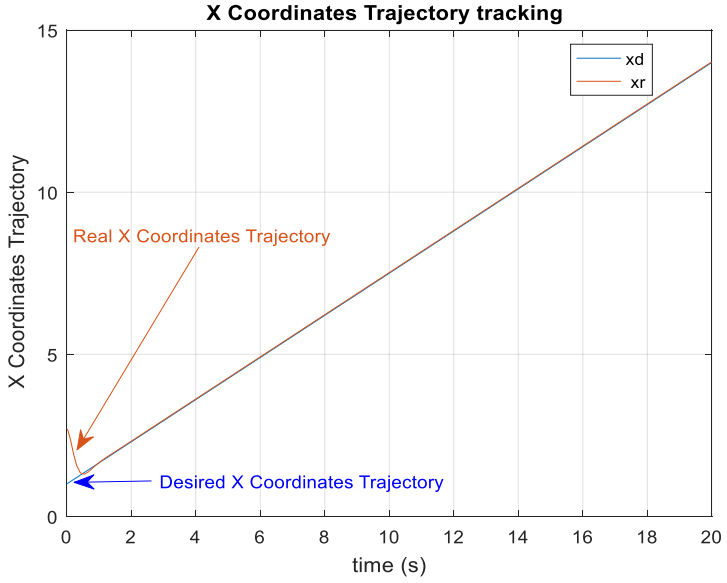

Figure 7: Desired and real Xc.

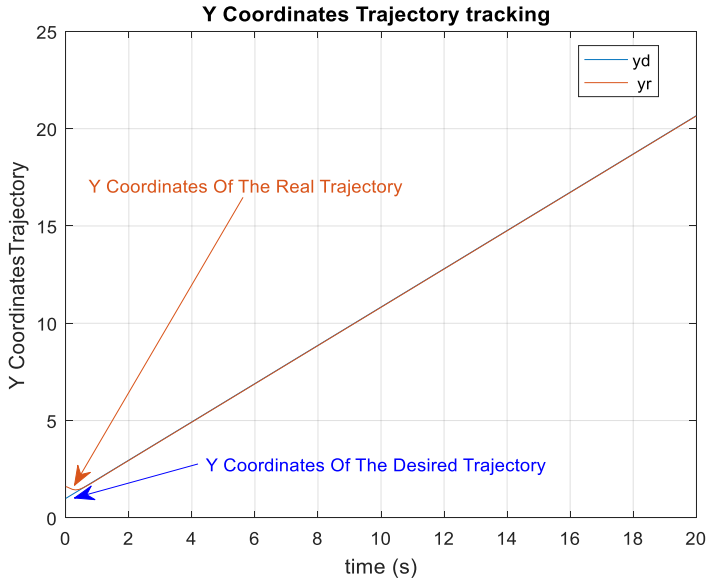

Figure 8: Desired and real Yc.

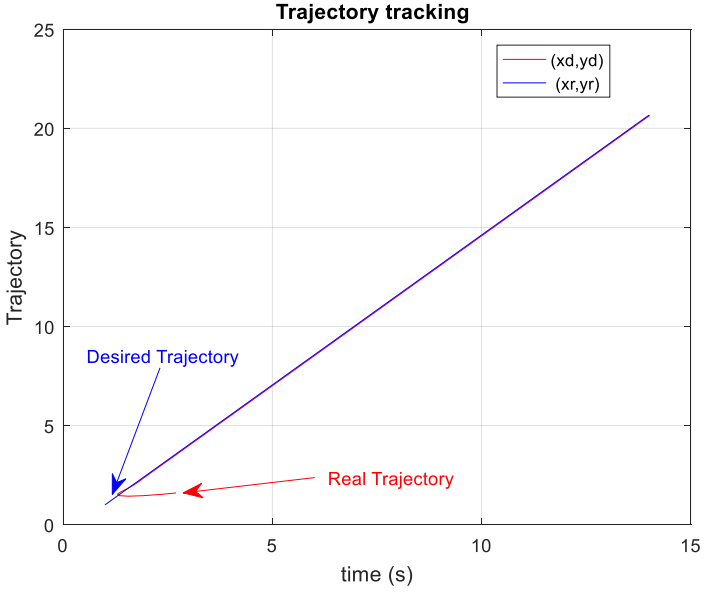

Figure 9: Desired and real trajectory.

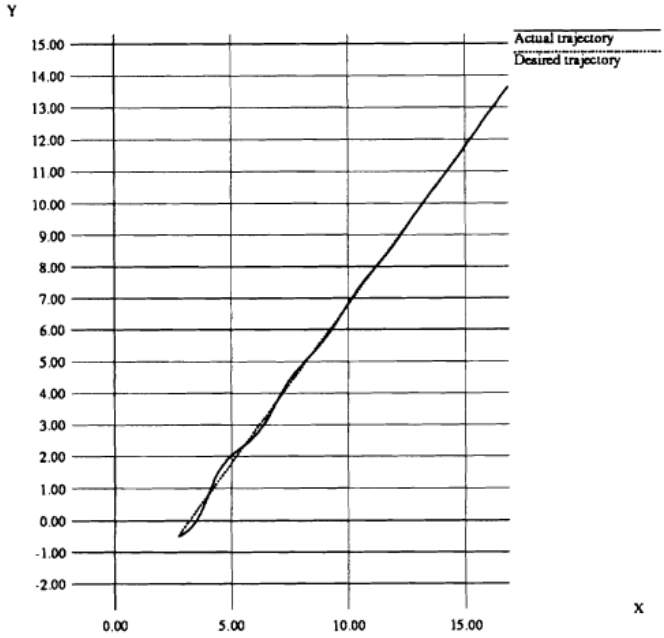

Figure 10: Desired and real trajectory (PD).

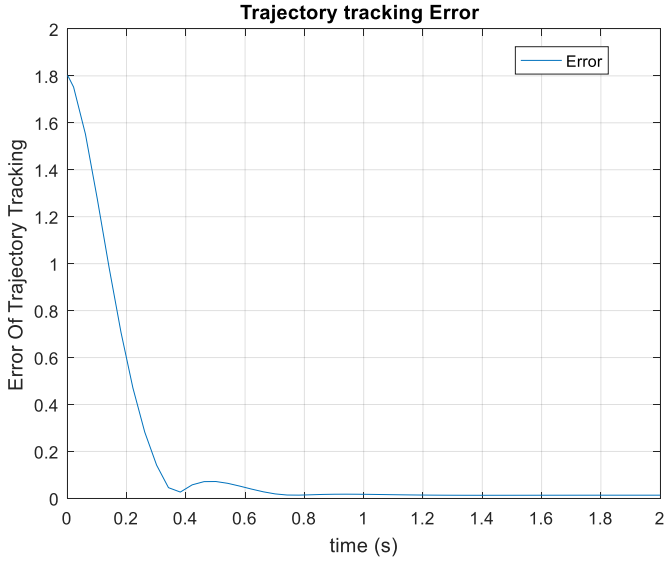

Figure 11: Trajectory tracking error.

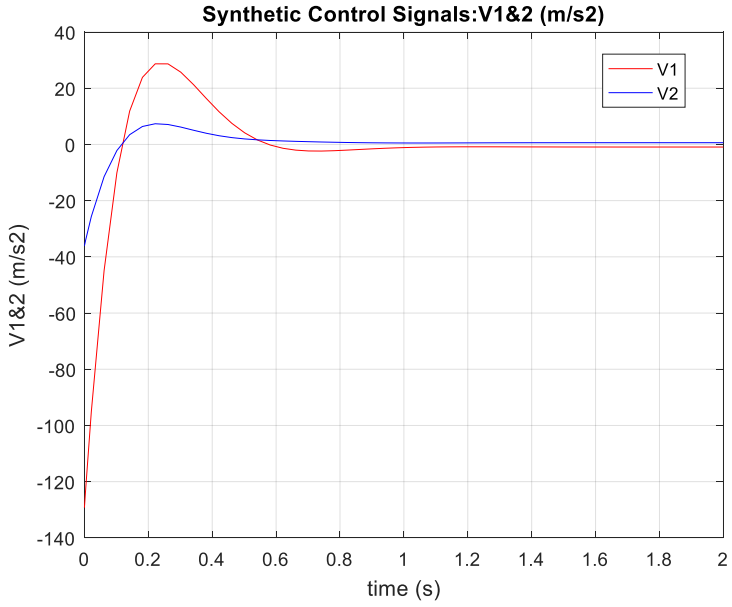

Figure 12: DDMR Synthetic control.

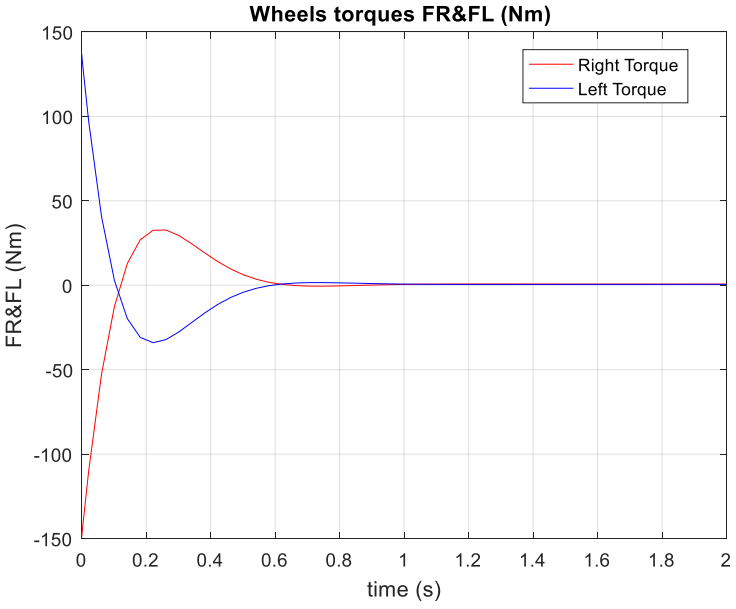

Figure 13: Wheels' driving torques.

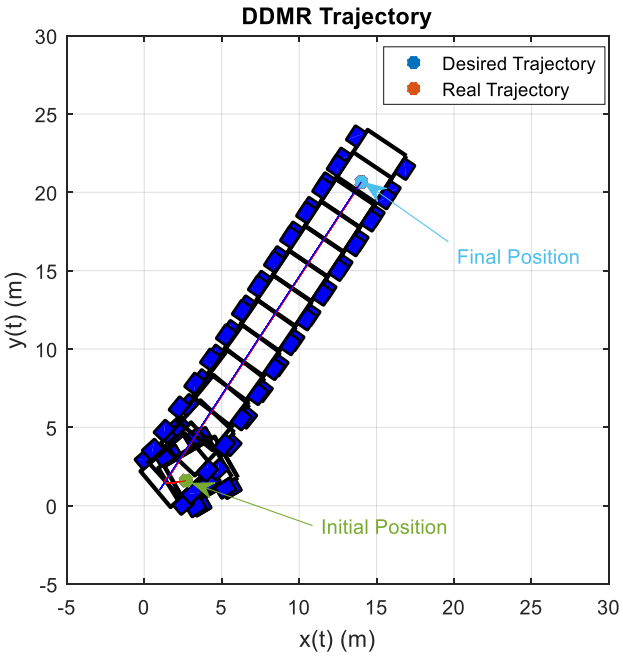

Figure 14: DDMR trajectory simulation.

Fig.7, 8 and *9* represent the trajectory of the Xc and Yc coordinates of the DDMR, from the initial to the final position; we notice fast asymptotic convergence of the two coordinates without oscillations comparing with *Fig. 10*, Yoshio and Xiaoping work [15], and the imposed settling time $T_{r\pm 5\%}$ limit (less than 1s) is respected. *Fig.11* shows the convergence of the trajectory tracking error towards a very small value. using the proposed control approach. In *Fig.12* the DDMR synthetic controls v_1, v_2 given by (39) are shown. As we can notice, the synthetic controls do converge almost to zero. *Fig.13* shows that the DDMR torques τ_1, τ_2 that can be obtained from the synthetic controls using (33), respect the imposed torque limitations $\tau_{i\,\max} \leq 150$. The *Fig. 14*, shows that the DDMR follows the desired trajectory rapidly without any overshoot or oscillations.

5. Conclusion

The present article proposes a model predictive control for a DDMR. The control strategy started with an input–output linearization technique to linearize the nonlinear dynamic model of the DDMR, then, based on the obtained linear

model, a predictive control law was developed. The prediction horizon time h and the weight factor ρ were tuned based on torques and settling time graphics analysis; the simulation results showed that we could find a trade-off between the settling time and the energy required for the mobile robot to follow the desired trajectory. In addition, the proposed approach produces a better system performance than the PD control technique proposed by Yoshio and Xiaoping [15]. Future work aims to apply this control law in discrete form, to a mobile manipulator robot with a high degree of freedom and challenge the obtained control law to follow a more complicated predefined trajectory. After that, the validation of the proposed approach on a real robot is envisaged.

Acknowledgements

This work was supported by the Ministry of Higher Education and Scientific Research of Algeria (CNEPRU J0201620140014).

The authors would like to thank the reviewers for their valuable comments.

References

[1] Guechi, E.H., Abellard, A., and Abellard, P. "TS-Fuzzy Predictor Observer Design for TrajectoryTracking of Wheeled Mobile Robot", IECON 2011-37th annual Conf. of IEEE Industrial Electronic Society, pp. 319–324, 2011.

[2] Guechi, E. H., Bouzoualegh, S., Messikh, L. and Blažic, S. "Model Predictive Control of a two-link robot arm", 2018 Int. Conf. on Advanced Sys. and Electric Tech. (IC_ASET), Tunisia, pp. 409–414, March 2018.

[3] Belda, K. and Rovný, O. "Predictive Control of 5 DOF Robot Arm of Autonomous Mobile Robotic System", In Proc. Process Control (PC), 2017 21st International Conference on IEEE, 2017.

[4] Kamel, M. and Zhang, Y. "Linear Model Predictive Control via Feedback Linearization for Formation Control of Multiple Wheeled Mobile Robots", Information and Automation, 2015 IEEE International Conference on. IEEE, pp. 1283–1288, Aug. 2015.

[5] Guechi, E. H., Bouzoualegh, S., Zennir, Y. and Blažic, S. "MPC Control Study and LQ Optimal Control of A Two-Link Robot Arm:A Comparative Study", Machines 2018, vol. 6, no. 3, pp. 37.

[6] Elkhateeb, N. A. and Badr, R. I. "Novel PID Tracking Controller for 2DOF Robotic Manipulator System Based on Artificial Bee Colony Algorithm", Electrical, Control and Communication Engineering, vol. 13, no.1 pp. 55–62, Dec. 2017.

[7] Mendili, M. and Bouani, F. "Predictive Control Based on Dynamic Modeling of OmniDir Mobile", Engineering & MIS (ICEMIS), 2017 International Conference on IEEE, pp. 1–6, May 2017.

[8] Mendili, M. and Bouani, F. "Predictive Control of Mobile Robot Using Kinematic and Dynamic Models", Hindawi, Journal of Control Science and Eng., vol. 2017.

[9] Maniatopoulos, S., Panagou, D. and Kyriakopoulos, K. J. "Model Predictive Control for the Navigation of a Nonholonomic Vehicle with Field-of-View Constraints", American Control Conference (ACC), 2013. IEEE, pp. 3967–3972, June 2013.

[10] Sinaeefar, Z. and Farrokhi, M. "Adaptive Fuzzy Model Based Predictive Control of Nonholonomic Wheeled Mobile Robots Including Actuators Dynamics", Int. Journal of Scientific & Eng. Research, vol. 3, no. 9, Sep. 2012.

[11] Mazur, A. "Hybrid adaptive control laws solving a path following problem for Non-Holonomic mobile manipulators", International Journal of Control, vol. 77, no. 15, pp. 1297–1306, Feb. 2007.

[12] Ostafew, C. J., Schoellig, A. P. and Barfoot, T. D. "Learning-Based Nonlinear MPC to Improve Vision-Based Mobile Robot Path Tracking", Journal of Field Robotics, vol. 33, no 1, pp. 133–152, 2016.

[13] Mitrovic, S. T., & Djurovic, Z. M. "Fuzzy-Based Controller for Differential Drive Mobile Robot Obstacle Avoidance", IFAC Proceedings, vol. 43, no. 16, pp. 67–72, 2010.

[14] Dhaouadi, R., & Hatab, A. A. "Dynamic modelling of differential drive mobile robots, a unified framework", Advances in Robotics & Automation, vol. 2, no. 2, pp. 1–7, 2013.

[15] Yamamoto, Y. and Yun, X. "Coordinating Locomotion and Manipulation of a Mobile Manipulator", Decision and Control, Proceedings of the 31st IEEE Conference, pp. 2643–2648, 1992.

[16] Magni, L., Scattolini, R. and Aström, K. J. "Global stabilization of the inverted pendulum using model predictive control", Proceedings of the 15th IFAC World Congress, vol. 1554, 2002.

[17] Gawthrop, P. J. and Wang, L. "Intermittent predictive control of an inverted pendulum", Control Engineering Practice, vol. 14, no. 11, pp. 1347–1356, 2006.

[18] Mills, A., Wills, A. and Ninness, B. "Nonlinear model predictive control of an inverted pendulum", Proceedings of the American Control Conference, pp. 2335–2340, 2009.

[19] MIT Open Course Ware,"Dynamics and Control", Spring 2008.